Phys. Status Solidi B **246**, No. 6, 1286–1290 (2009) / **DOI** 10.1002/pssb.200844322

physica status solidi b
www.pss-b.com
basic solid state physics

Spin-decoherence effects on the pumped spin-dependent transport through a quantum dot

Hui Pan[*,1], **Zheng Li**[1], **Su-Qing Duan**[2], **Wei-Dong Chu**[2], **and Wei Zhang**[2]

[1] Department of Physics, Beijing University of Aeronautics and Astronautics, Beijing 100083, P.R. China
[2] Institute of Applied Physics and Computational Mathematics, Beijing 100088, P.R. China

Received by C. S. Lee 7 August 2008, revised 16 December 2008, accepted 19 December 2008
Published online 23 February 2009

PACS 73.23.Hk, 73.63.Kv, 76.30.Pk, 85.75.–d

[*] Corresponding author: e-mail hpan@buaa.edu.cn

We theoretically study the spin-decoherence effects on the pumped spin-polarized current through a quantum dot subject to a rotating magnetic field and coupled to two ferromagnetic electrodes. The dependence of the current on the magnetic moment orientation angle of the two leads is greatly influenced by the spin pump and the spin decoherence. The spin pump destroys the normal spin-valve effects, and the spin decoherence makes the current exhibiting a quite complicated angle dependence. These distinct transport behaviors can be used as electrical schemes for detection of electron spin resonance and spin decoherence. Moreover, the current is closely related to the magnetic Rabi frequency and the detuning, in which the spin decoherence also plays an important role, and thus the pumped spin-polarized current can be used as a sensitive tool to measure these pumping parameters.

1 Introduction Spin-dependent electronic transport in quantum dot (QD) systems has attracted extensive investigations, since it provide the way for applications in spintronics and quantum information processing [1, 2]. The transport through a QD coupled to ferromagnetic leads strongly depends on the magnetic configuration of the system [3–5], since they affect the polarization of the electronic current and so the magnitude of current. In the QD systems of nanometer length scale, the Coulomb blockade (CB) of the single-electron tunneling is a fundamental physical phenomenon at low temperatures. In the spin-polarized transport, the strong Coulomb interactions can result in a zero-bias anomaly in the Coulomb-blockade valleys [6–8]. Recently, the spin-polarized electronic transport through a QD under an external magnetic field perpendicular to the magnetizations of two leads has been studied [9, 10]. A new phenomenon of Coulomb promotion of spin-dependent tunneling has been proposed, which arises from combined effects of spin-flip processes induced by the magnetic field and Coulomb correlations.

On the other hand, coherent control of spin dynamics in a QD using a rotating magnetic field in a solid-state environment has been a subject of increasing interest in recent years [11], because it has been a very important problem of spintronics to understand and exploit various physical mechanisms for generating spin current in solid-state devices. This interest has led to a large amount of work on detection of the electron spin resonance (ESR) in a QD [12, 13]. A spin-source device has been proposed to carry pure spin flow based on ESR in single or coupled QD systems with sizable Zeeman splitting [14–16]. However, the controlling of the spin-dependent electronic transport through an interacting QD attached to ferromagnetic (FM) leads by a rotating magnetic field are still less studied. The ESR effect on the spin-dependent transport through the QD needs investigations, since the spin configuration of the confined electrons in QD is apparently affected by ESR effect, which directly determines the efficiency of this device. In addition, the previous studies also neglected the inevitable spin decoherence due to coupling of the single spin with environment [17–19].

Therefore, it is the purpose of this paper to study the ESR-pumped spin-polarized current for a QD connected with two FM leads in the strong CB regime. The magnetization of the left lead is presumed to align along the $\hat{z}$-axis, and the magnetization of the right lead is supposed to deviate from the $\hat{z}$-axis by an angle θ. The spin pump is facilitated by a rotating magnetic field which induces the spin-flip effects. By using the quantum rate equations, we have predicted that the spin-polarized current can be easily controlled by tuning the rotating magnetic field. In the absence of the rotating magnetic field, the spin-polarized current decreases monotonically from $\theta = 0$ to $\theta = \pi$, showing the normal spin-valve effect. However, in the presence of the rotating magnetic field, the current shows a reversed current-angle relation. Furthermore, due to the finite spin decoherence time T_c, the current shows a nonmonotonic variation with the angle θ. Therefore, these distinct transport behaviors can be used as electrical schemes for detection of electron spin resonance and spin decoherence.

The rest of this paper is organized as follows. In Section 2 we present the model Hamiltonian and derive the formula of the spin-dependent electronic current by using the the quantum rate equations. In Section 3 we study the spin-polarized current by tuning various parameters. Finally, a brief summary is given in Section 4.

2 Physical model and formula The FM–QD–FM system with a rotating magnetic field is described by the following Hamiltonian:

$$H = \sum_{\eta=\mathrm{L,R}} H_\eta + H_{\mathrm{dot}} + H'(t) + H_{\mathrm{T}}\,, \tag{1}$$

with

$$H_\eta = \sum_{k\sigma} \varepsilon_{\eta k\sigma} a^\dagger_{\eta k\sigma} a_{\eta k\sigma}\,, \tag{2}$$

$$H_{\mathrm{dot}} = \sum_{\sigma} \varepsilon_\sigma d^\dagger_\sigma d_\sigma + U n_\uparrow n_\downarrow\,, \tag{3}$$

$$H'(t) = R_{\mathrm{sf}}\, \mathrm{e}^{i\omega t}\, d^\dagger_\uparrow d_\downarrow + \mathrm{h.c.}\,, \tag{4}$$

$$H_{\mathrm{T}} = \sum_{k\sigma}\Bigg[t_{\mathrm{L}} a^\dagger_{\mathrm{L}k\sigma} d_\sigma + t_{\mathrm{R}}\left(\cos\frac{\theta}{2}\, a^\dagger_{\mathrm{R}k\sigma} d_\sigma - \sigma \sin\frac{\theta}{2}\, a^\dagger_{\mathrm{R}k\bar{\sigma}} d_\sigma\right) + \mathrm{h.c.}\Bigg]. \tag{5}$$

H_η ($\eta = \mathrm{L,R}$) describes the left and right ferromagnetic leads. The magnetic moment $\boldsymbol{M}$ of the left electrode is pointing to the $\hat{z}$-direction, the electric current is flowing in the $\hat{x}$-direction, while the moment of the right electrode is at an angle θ to the $\hat{z}$-axis in the $\hat{y},\hat{z}$-plane. We have made a simplification that the value of molecular field M is the same for the two FM leads, thus the spin-valve effect is obtained by varying the angle θ [14, 20]. H_{dot} models the quantum dot where $d^\dagger_\sigma$ (d_σ) represents the creation (annihilation) operator of the electron with energy ε_σ and spin $\sigma = \pm 1 = \uparrow\downarrow$ ($\bar{\sigma} = -\sigma$). The dot energy is assumed to be independent of the bias voltage. The field rotates around $\hat{z}$- axis with a tilt angle φ as: $\boldsymbol{B}(t) = (B_0 \sin\varphi\cos\omega t,\ B_0 \sin\varphi \sin\omega t,\ B_0\cos\varphi)$, where B_0 is the constant magnetic field strengths. The rotating components $(B_0 \sin\varphi\cos\omega t,\ B_0 \sin\varphi\sin\omega t)$ in the $\hat{x},\hat{y}$-plane provide a spin flip mechanism. The $\hat{z}$ component $B_z = B_0\cos\varphi$ gives the Zeeman splitting. The single-electron level in the QD is split into $\Delta = \varepsilon_\downarrow - \varepsilon_\uparrow = \mu_{\mathrm{B}} B_0 \cos\varphi$, where μ_{B} is the Bohr magneton. U is the on-site Coulomb repulsion, and $n_\sigma = d^\dagger_\sigma d_\sigma$ is the particle number operator. H' is the off diagonal part of the Hamiltonian with $R_{\mathrm{sf}} = \mu_{\mathrm{B}} B_0 \sin\varphi$ describing the spin-flip scattering caused by the rotating magnetic field. H_{T} represents the tunneling coupling between the QD and leads, and the tunneling matrix element is set as t_η.

Due to the strong Coulomb interaction in the QD, the double occupation is prohibited. Here, in order to anticipate the CB and the intrinsic spin relaxation, we utilize the quantum rate equations to solve for the system density matrix elements. The unoccupied and spin states are ρ_0 and ρ_σ, which describe the occupation probability in the QD. The off-diagonal term $\rho_{\sigma\sigma'}$ denotes coherent superposition of the two coupled spin states in the QD. The doubly occupied state ρ_2 is prohibited due to the strong Coulomb interaction U. Here we focus our interest on the nonadiabatic pumping where the photon-assisted resonance is achieved. The quantum rate equations for the spin-resolved density matrix elements in the rotating frame with respect to ω are ($e = \hbar = 1$)

$$\begin{aligned}
\frac{\mathrm{d}\rho_0}{\mathrm{d}t} &= -\Gamma^+_\uparrow \rho_0 - \Gamma^+_\downarrow \rho_0 + \Gamma^-_\uparrow \rho_\uparrow + \Gamma^-_\downarrow \rho_\downarrow\,,\\
\frac{\mathrm{d}\rho_\uparrow}{\mathrm{d}t} &= \Gamma^+_\uparrow \rho_0 - \Gamma^-_\uparrow \rho_\uparrow + iR_{\mathrm{sf}}(\rho_{\uparrow\downarrow} - \rho_{\downarrow\uparrow})\,,\\
\frac{\mathrm{d}\rho_\downarrow}{\mathrm{d}t} &= \Gamma^+_\downarrow \rho_0 - \Gamma^-_\downarrow \rho_\downarrow + iR_{\mathrm{sf}}(\rho_{\downarrow\uparrow} - \rho_{\uparrow\downarrow})\,,\\
\frac{\mathrm{d}\rho_{\uparrow\downarrow}}{\mathrm{d}t} &= -\frac{1}{2}(\Gamma^-_\uparrow + \Gamma^-_\downarrow)\,\rho_{\uparrow\downarrow} + i\delta_{\mathrm{ESR}}\rho_{\uparrow\downarrow} + iR_{\mathrm{sf}}(\rho_\uparrow - \rho_\downarrow) - \frac{1}{T_c}\rho_{\uparrow\downarrow}\,,\\
\frac{\mathrm{d}\rho_{\downarrow\uparrow}}{\mathrm{d}t} &= -\frac{1}{2}(\Gamma^-_\downarrow + \Gamma^-_\uparrow)\,\rho_{\downarrow\uparrow} - i\delta_{\mathrm{ESR}}\rho_{\downarrow\uparrow} + iR_{\mathrm{sf}}(\rho_\downarrow - \rho_\uparrow) - \frac{1}{T_c}\rho_{\downarrow\uparrow}\,,
\end{aligned} \tag{6}$$

and the normalization relation $\rho_0 + \rho_\uparrow + \rho_\downarrow = 1$. In these equations, $\delta_{\mathrm{ESR}} = \Delta - \omega$ is the ESR detuning. Furthermore, we describe the coupling of single spin with the environment in a phenomenological way via introducing the spin decoherence time scale T_c, which is related to the loss of phase coherence of the spin superposition state. [15] The measurement of T_c in QDs is currently an active topic be-

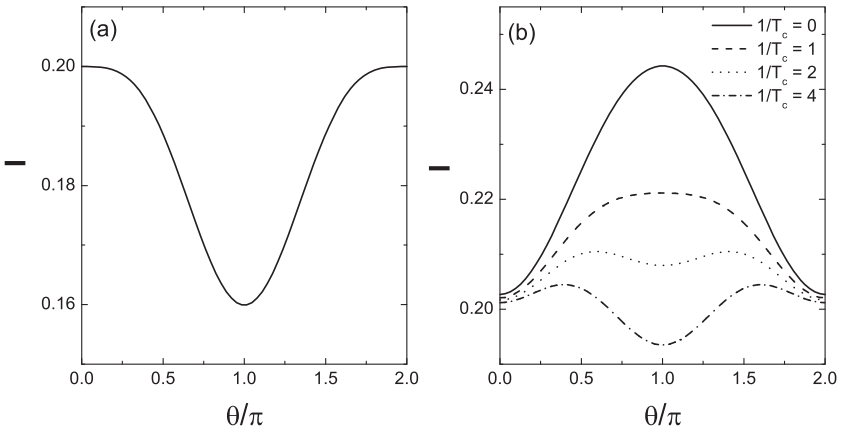

Figure 1 I versus θ for (a) $R_{\rm sf}=\omega=0$ and (b) $R_{\rm sf}=0.5$ and $\omega=2.0$ with different $T_{\rm c}$. Other parameters are $\varepsilon_{\downarrow}=2.0$, $\varepsilon_{\uparrow}=0$, and $V=5.0$.

cause it is the limit time scale for coherent spin manipulation and thus quantum information processing.

The parameter $\Gamma_{\sigma}^{+}=\sum_{\eta=\mathrm{L,R}}\Gamma_{\eta\sigma}^{+}$ corresponds to the rate of adding one electron to the dot coming from the leads, and $\Gamma_{\sigma}^{-}=\sum_{\eta=\mathrm{L,R}}\Gamma_{\eta\sigma}^{-}$ is the rate of moving one electron from the dot to the leads. Due to the FM leads, the tunneling rates are

$$\Gamma_{\mathrm{L}\sigma}^{+}=\Gamma_{\mathrm{L}\sigma}f_{\mathrm{L}}\,, \tag{7}$$

$$\Gamma_{\mathrm{L}\sigma}^{-}=\Gamma_{\mathrm{L}\sigma}(1-f_{\mathrm{L}})\,, \tag{8}$$

$$\Gamma_{\mathrm{R}\sigma}^{+}=(\Gamma_{\mathrm{R}\sigma}\cos^{2}\theta+\Gamma_{\mathrm{R}\bar{\sigma}}\sin^{2}\theta)\,f_{\mathrm{R}}\,, \tag{9}$$

$$\Gamma_{\mathrm{R}\sigma}^{-}=(\Gamma_{\mathrm{R}\sigma}\cos^{2}\theta+\Gamma_{\mathrm{R}\bar{\sigma}}\sin^{2}\theta)\,(1-f_{\mathrm{R}})\,, \tag{10}$$

where $f_{\eta}(\varepsilon)=1/(\mathrm{e}^{(\varepsilon-\mu_{\eta})/k_{\mathrm{B}}T}+1)$ denotes the Fermi distribution function of electrons in the η lead. The chemical potentials are set as $\mu_{\mathrm{L}}=\mathrm{eV}$ and $\mu_{\mathrm{R}}=0$ with eV the bias. The coupling between the QD and the lead η is related to the spin-resolved density of states of lead η via $\Gamma_{\eta\sigma}=2\pi\rho_{\eta\sigma}t_{\eta\sigma}^{*}t_{\eta\sigma}$. With the definition of the spin polarization of η lead $p_{\eta}=(\rho_{\eta\uparrow}-\rho_{\eta\downarrow})/(\rho_{\eta\uparrow}+\rho_{\eta\downarrow})$, the coupling can be expressed as $\Gamma_{\eta\sigma}=\Gamma_{0}(1\pm p_{\eta})$ with $\Gamma_{0}=(\Gamma_{\eta\uparrow}+\Gamma_{\eta\downarrow})/2$. The linewidth function Γ_{0} is set as small value compared with the energy-level spacing for the symmetric and weak-coupling case. In wide band limit, these tunneling amplitudes are independent of energy. The current from the η lead to the central region can be calculated from standard rate equations, which yield

$$I_{\eta\sigma}=\Gamma_{\eta\sigma}^{+}\rho_{0}-\Gamma_{\eta\sigma}^{-}\rho_{\sigma}\,, \tag{11}$$

The total current is $I=(1/2)\,(I_{\mathrm{L}}-I_{\mathrm{R}})$ with $I_{\eta}=I_{\eta\uparrow}+I_{\eta\downarrow}$. The spin-polarization of the two FM leads are set as $p_{\mathrm{L}}=p_{\mathrm{R}}=0.3$, and the temperature is set as zero. The linewidth function $2\Gamma_{0}=\Gamma_{\eta\uparrow}+\Gamma_{\eta\downarrow}=1$ is set as the energy unit, whose typical values are of the order of tens of μeV [21].

3 Numerical results and discussions To clearly show the spin-pump effects on spin-polarized current, I versus θ without and with a rotating magnetic field is plotted in Fig. 1(a) and (b), respectively. In the absence of the magnetic field, the θ dependence of the tunneling current exhibits the normal spin-valve effect [22, 23]. The current arrives at its maximum and minimum in the parallel ($\theta=2n\pi$) and antiparallel magnetization configurations [$\theta=(2n+1)\,\pi$], respectively. The current exhibits a monotonic change in between the parallel and antiparallel magnetization configurations. However, in the presence of the rotating magnetic field, the current is reversed and

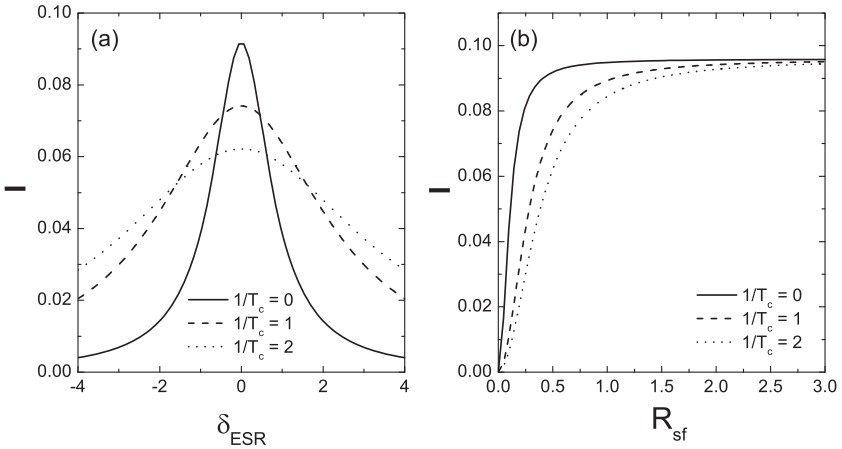

Figure 2 I versus (a) δ_{ESR} at $R_{\rm sf}=0.5$ and (b) $R_{\rm sf}$ at $\omega=2$ with different $T_{\rm c}$. Other parameters are $\varepsilon_{\downarrow}=1.0$, $\varepsilon_{\uparrow}=-1.0$, and $V=5.0$.

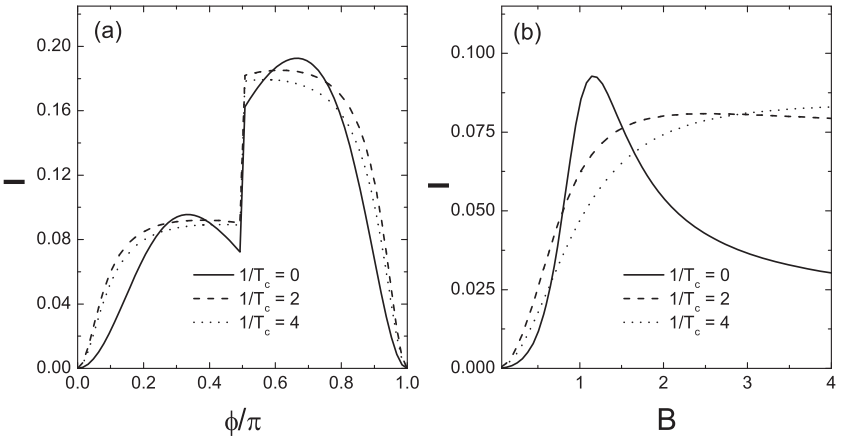

Figure 3 I versus (a) φ at $B_0 = 2$ and (b) B at $\varphi = \pi/6$ with different T_c. Other parameters are $\omega = 2$ and $V = 5.0$.

arrives at its maximum and minimum in antiparallel $[\theta = (2n+1)\pi]$ and the parallel $(\theta = 2n\pi)$ magnetization configurations, respectively. The reason is related to the spin-pump effects caused by the external rotating magnetic field. After a spin-up electron tunnels into the QD from the left FM, an oscillating magnetic field applied with the frequency nearly equal to Δ can pump the electron to the higher level where its spin is flipped, then the spin-down electron can tunnel out to the right FM lead. Therefore, the spin-pump effects cause the reversion of the I–θ relation.

The inevitable spin decoherence due to coupling of the single spin with environment can not be fully neglected. The spin decoherence does not influence the I–θ relation at zero magnetic field. However, the decoherence has a distinct influence on the I–θ relation when a rotating magnetic field is applied as shown in Fig. 1(b). With increasing $1/T_c$, the current peak at $\theta = \pi$ decreases and finally a dip appears, showing a nonmonotonic relation with θ in the presence of magnetic field. The nonmonotonic behavior comes from the competition between the spin-decoherence and the spin-pump effects, since the shorter spin-decoherence time can result in the sooner loss of phase coherence of the spin superposition state.

Figure 2 shows the controlling of the current by the detuning δ_{ESR} and Rabi frequency R_{sf} of the magnetic field. As shown in Fig. 2(a), the current reaches its maximum value at zero detuning of $\delta_{ESR} = 0$ as expected, where a resonance appears. With increasing $1/T_c$, the maximum current decrease and its width becomes wider due to the shorter decoherence time. The detailed dependence of the current on the driving frequency is determined by the spin-decoherence time T_c. Figure 2(b) shows that the current amplitude exhibits a saturation behavior with increasing Rabi frequency R_{sf}. This is a consequence of the photon absorption of a single spin, and the saturated value is independent of the decoherence time T_c and detuning δ_{ESR}. The curves become steeper at larger $1/T_c$.

Finally, we study effects of the external field angle φ and strength B on the current. As shown in Fig. 3(a), the current shows a sudden increase at $\varphi = \pi/2$. The reason is related to the spin-pump effects and the spin polarization of the FM leads. When $\varphi < \pi/2$, the Zeeman splitting is $\Delta = \varepsilon_\downarrow - \varepsilon_\uparrow = \mu_B B_0 \cos\varphi > 0$. The spin-up electrons from the left lead can be flipped from the state $\varepsilon_\uparrow$ to the state $\varepsilon_\downarrow$ and then tunnel to the right lead with tunneling rate $\Gamma_{R\downarrow}$. When $\varphi > \pi/2$, the Zeeman splitting becomes $\Delta = \varepsilon_\downarrow - \varepsilon_\uparrow = \mu_B B_0 \cos\varphi < 0$. The spin-down electrons from the left lead can be flipped to the state $\varepsilon_\uparrow$ and then tunnel to the right lead with tunneling rate $\Gamma_{R\uparrow}$. Due to the nonzero spin polarization $p_R = 0.3$ of the FM lead, the tunneling rate is $\Gamma_{R\uparrow} = \Gamma_0(1+p_R) > \Gamma_{R\downarrow} = \Gamma_0(1-p_R)$. Thus the current $I(\varphi)$ with $\pi/2 < \varphi < \pi$ is larger than $I(\pi-\varphi)$. This explains the increase of the current when φ sweeps $\pi/2$. The current peak in the range $\varphi < \pi/2$ or $\varphi > \pi/2$ is caused by the resonance as mentioned above. When the decoherence time T_c decreases, the two resonant peaks smears slowly due to the spin relaxation. The current versus the magnetic field strength B is plotted in Fig. 3(b) at different φ. It is seen that the resonant peak appears at the same B for φ and $\pi - \varphi$, since the resonance happens at $\omega = \Delta = g\mu_B B_0 \cos\varphi$. Similarly, the resonant peak is smeared by increasing $1/T_c$. It is also a way to detect the spin decoherence time.

4 Summary In summary, based on the quantum rate equation, we have studied the spin-decoherence effects on the pumped spin-polarized current through the quantum dot subject to a rotating magnetic field and coupled to two ferromagnetic electrodes. Our results show that the dependence of the current on the magnetic moment orientation angle θ of the two leads is greatly influenced by the spin-pump effects and the spin decoherence. The ESR pumping generates a reversed dependence of the current on the magnetic moment orientation angle θ. Furthermore, the current displays a quite complicated behavior depending on θ under the influence of the spin decoherence time T_c. Therefore, these distinct transport behaviors can be used as electrical schemes for detection of ESR and spin decoherence. The current also depends on the magnetic Rabi frequency and the detuning sensitively, in which the spin-decoherence also plays an important role, and thus the pumped spin-polarized current can be used as a sensitive tool to measure these pumping parameters.

Acknowledgments This work is supported by the National Natural Science Foundation of China (Grant No. 10704005) and the Beijing Municipal Science and Technology Commission (Grant No. 2007B017).

References

[1] S. A. Wolf, D. D. Awschalom, R. A. Buhrman, J. M. Daughton, S. von Molnar, M. L. Roukes, A. Y. Chtchelka, and D. M. Treger, Science **294**, 1488 (2001).
[2] I. Zutic, J. Fabian, and S. Das Sarma, Rev. Mod. Phys. **76**, 323 (2004).
[3] J. König and J. Martinek, Phys. Rev. Lett. **90**, 166602 (2003).
[4] H. Pan and T. H. Lin, Phys. Lett. A **360**, 317 (2006).
[5] W. Rudzinski et al., Phys. Rev. B **64**, 085318 (2001).
[6] S. Braig and P. W. Brouwer, Phys. Rev. B **71**, 195324 (2005).
[7] I. Weymann, J. Barnaś, J. König, J. Martinek, and G. Schön, Phys. Rev. B **72**, 113301 (2005).
[8] I. Weymann and J. Barnaś, Phys. Rev. B **75**, 155308 (2007).
[9] L. Y. Gorelik, S. I. Kulinich, R. I. Shekhter, M. Jonson, and V. M. Vinokur, Phys. Rev. Lett. **95**, 116806 (2005).
[10] Y. Q. Zhou, R. Q. Wang, B. Wang, and D. Y. Xing, Phys. Rev. B **76**, 075343 (2007).
[11] M. Grifoni and P. Hänggi, Phys. Rep. **304**, 229 (1998).
[12] M. Xiao, I. Martin, E. Yablonovitch, and H. W. Jiang, Nature (London) **430**, 435 (2004).
[13] O. Gywat, H. A. Engel, D. Loss, R. J. Epstein, F. M. Mendoza, and D. D. Awschalom, Phys. Rev. B **69**, 205303 (2004).
[14] B. Wang, J. Wang, and H. Guo, Phys. Rev. B **67**, 092408 (2003).
[15] B. Dong, H. L. Cui, and X. L. Lei, Phys. Rev. Lett. **94**, 066601 (2005).
[16] H. Pan, S. Q. Duan, L. N. Zhao, W. D. Chu, and W. Zhang, Eur. Phys. J. B **62**, 71 (2008).
[17] A. V. Khaetskii, D. Loss, and L. Glazman, Phys. Rev. Lett. **88**, 186802 (2002).
[18] K. A. Al-Hassanieh, V. V. Dobrovitski, E. Dagotto, and B. N. Harmon, Phys. Rev. Lett. **97**, 037204 (2006).
[19] R. Hanson, L. P. Kouwenhoven, J. R. Petta, S. Tarucha, and L. M. K. Vandersypen, Rev. Mod. Phys. **79**, 1217 (2007).
[20] J. C. Slonczewski, Phys. Rev. B **39**, 6995 (1989).
[21] A. Kogan, S. Amasha, D. Goldhaber-Gordon, G. Granger, M. A. Kastner, and H. Shtrikman, Phys. Rev. Lett. **93**, 166602 (2004).
[22] M. Braun, J. König, and J. Martinek, Phys. Rev. B **70**, 195345 (2004),
[23] I. Weymann, J. König, J. Martinek, J. Barnaś, and G. Schön, Phys. Rev. B **72**, 115334 (2005).

